An Experimental Study on the Characteristics of Vertical Acceleration on Small High Speed Craft in Head Waves

Toru, Katayama, *Graduate School of Engineering, Osaka Prefecture University*

katayama@marine.osakafu-u.ac.jp

Ryosuke, Amano, *Graduate Student, Graduate School of Engineering, Osaka Prefecture University*

sv103001@edu.osakafu-u.ac.jp

ABSTRACT

In this study, the characteristics of vertical acceleration on small high speed passenger craft in head waves are investigated experimentally, an empirical method to estimate it is proposed. First, how to decide the sampling frequency and the test duration (total number of waves encounters) is discussed to measure acceleration accurately. Next, the vertical acceleration on a hull is measured in regular and irregular waves, and the characteristics of the vertical acceleration for wave height, wave period and forward speed are investigated. And its probability density function is also investigated for the results in irregular waves. Moreover, the same measurements for two different hulls are carried out, and the effects of hull form is investigated.

Keywords: *vertical acceleration, small high craft, irregular waves*

1. INTRODUCTION

Recently, the maximum forward speed of small passenger craft is increasing. In case of the craft, the encounter wave period becomes shorter with increase of forward speed, and very large upward vertical acceleration is caused when its bow goes into the water surface. It is known that it cause not only bad ride comfort but also failure of hull or injury of passengers in some cases.

For development hull form, it is necessary to estimate the response of acceleration for its forward speeds and sea conditions. And for safety navigation management, it is important to estimate statistical short-term prediction of occurrence of un-desired large vertical acceleration.

The purpose of this study is to investigate the above-mentioned characteristics of vertical acceleration of small high speed passenger craft. First, in order to measure accurate vertical acceleration by a partly captive model test, data sampling and data analysis methods are discussed. Next, the vertical acceleration on a hull is measured in regular and irregular waves, and the characteristics of the vertical acceleration for wave height, wave period and forward speed are investigated. And its probability density function is also investigated for the results in irregular waves. Moreover, the same measurements for two additional

different hulls are carried out, and the effects of hull form is investigated.

2. OBJECT SHIP

Table 1 and Fig.1 show the principle particulars of models and their photographs. Fig.2 shows the body plan of Ship A. Their loading condition is full load. They are fast semi-planing craft with warped V and their draft is shallower and L_{pp}/B is larger than typical planing hulls. In the comparisons among the models, L_{pp}/B of Ship B is smaller than others and dead rise angle of Ship B is larger than others.

Table 1 Principal particulars of the models in real scale.

	Ship A	Ship B	Ship C
Scale: 1/S	1/23.4	1/21.0	1/21.0
Length between perpendiculars: L_{pp} [m]	23.4	14.95	18.1
Breadth: B [m]	4.5	4.5	4.4.
Deadrise angle at $s.s.$=5.0: β [deg]	18	18	24
Displacement: W [tonf]	36.76	25.91	31.51
Draft: d [m]	0.760	0.751	0.953

Fig.1 Photographs of the models (Ship A, B and C)

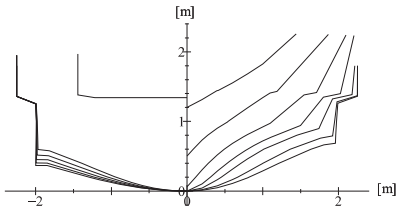

Fig.2 Body plan of the model (ship A).

3. MEASUREMENT AND ANALYSIS

3.1 Measuring device and coordinate system

Fig.2 show a schematic view of experiment and its coordinate system. Fig.3 shows its picture. A model is towed at constant speed with heaving and pitching free condition. And heaving (up: +), pitching (bow up: +) and normal acceleration on the base line of the hull (upward: +) are measured. Three acceleration sensors are installed on bow, midship and stern. Wave height is also measured with a servo type wave height meter attached to the towing carriage.

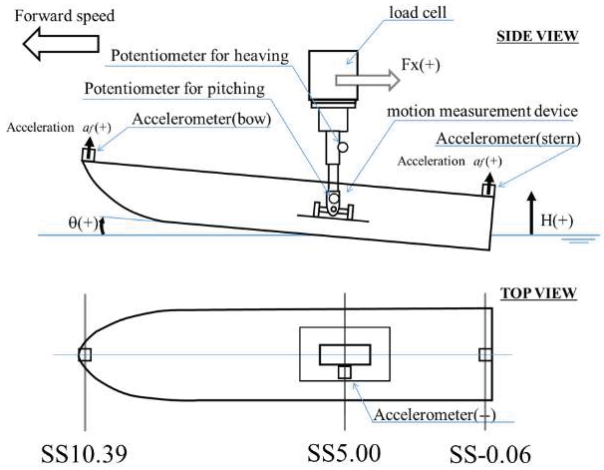

Fig.2 Schematic view of the experiment to measure vertical acceleration on hull

Fig.3 Photograph of the experiment.

3.2 Sampling frequencies

The sampling frequencies *fs* [Hz] in the measurement is decided by eq.(1).

$$fs_s \geq \frac{n_s}{\Delta t}\sqrt{s} \qquad (1)$$

where s is the denominator of scale of model, Δt [sec] is the shortest duration of impact accelerations acting on hull in irregular waves in real scale, n_s is the number of sampling data in the impact acceleration. According to the reference (National Maritime Research Institute, 2007 and Takemoto et al., 1981), Δt is about 120msec in real scale. To express the peak of the impact acceleration, if n_s = 4 or 5 (Seakeeping Committee of ITTC, 2011) is assumed, an adequate *fs* = 200Hz is obtained. Fig.4 shows the convergency of average amplitude of vertical acceleration measured for different sampling frequencies (100, 200, 500, 1000Hz). The number of encounter waves is more than 400.

The upper figure shows the average of upward peak value of the acceleration and the under one shows the average of downward peak value of the acceleration, and the horizontal axis is sampling frequency. As a result, it is noted that the margin of error is smaller than 5% when the number of sampling frequencies is more than 200Hz. Therefore, the number of sampling frequencies in the measurement is decided for 200Hz.

Fig.5 shows a time history of measured accleration at FP. In the measurement, the impact acceleration shown at t = 0.7seconds in Fig.5 is observed commonly in each measured data. The acceleration occurs when its bow goes down into the water surface. In order to obtain the peak to peak values of the acceleration, zero-down crossing method is used in the analysis. As seen in Fig.5, time history of measured acceleration has noise. To take zero cross points, the data filtered with a central moving average method of 10 datum is used. On the other hand, to take accurate peak value of the acceleration, the data filtered with a central moving average method of 2 datum is used.

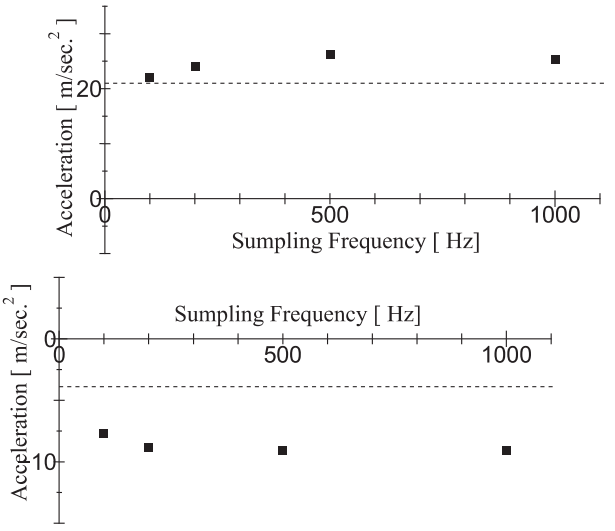

Fig.4 Variation of average of amplitude of vertical acceleration measured for different sampling frequencies. (upper figure: upward acceleration, lower figure: downward acceleration)

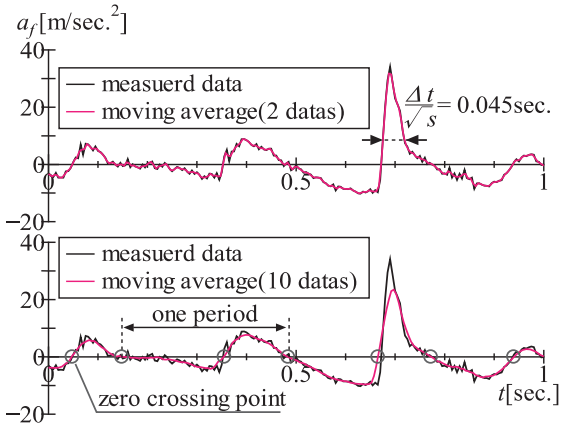

Fig.5 Time histories of measured data in irregular waves. (upper figure: a central moving average method of 2 datum, lower figure: a central moving average method of 10 datum)

3.3 Sampling number of encounter waves

Fig.6 shows the convergency of average amplitude of vertical acceleration measured for different sampling number of encounter waves. The upper figure shows the average of upward peak value of the acceleration and the under one shows the average of downward peak value of the acceleration, and the horizontal axis is sampling number of encounter waves. As a result, it is noted that the margin of error is smaller than ±4% when the sampling number of encounter waves is more than 200. Therefore, measurement in irregular waves is carried out with more than 200 encounter waves.

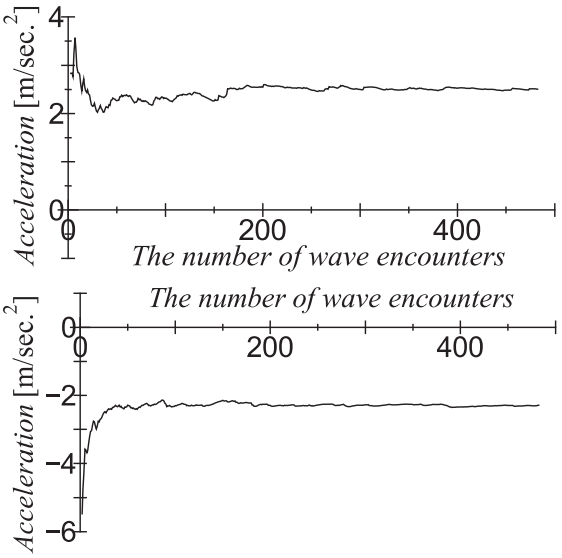

Fig.6 Variation of average of amplitude of measured vertical acceleration for numbers of amplitude data.(upper figure: upward peak value, lower figure: downward peak value)

3.4 Longitudinal distribution of vertical acceleration

The instantaneous acceleration a_X on longitudinal position X on hull is expressed as Eq.(2) with heaving and pitching of an arbitrary position.

$$a_X = \ddot{z}\cos\theta + l_X\ddot{\theta} + (1-\cos\theta)g \quad (2)$$

Where z is heave displacement (upward: +), θ is pitch angle (bow up: +), l_X is distance (forward:+) from the position of motion measuring and g is the gravitational acceleration (downward: +). Furthermore the heave and pitch accelerations are calculated with numerical differentiation of their data of displacement.

The accelerations measured on two different position on hull (a_A and a_F) are expressed as eq.(3) and eq.(4) by using eq.(2).

$$a_A = \ddot{z}\cos\theta + l_A\ddot{\theta} + (1-\cos\theta)g \quad (3)$$

$$a_F = \ddot{z}\cos\theta + l_F\ddot{\theta} + (1-\cos\theta)g \quad (4)$$

By using eq.(3) and eq.(4), heave and pitch terms in eq.(2) can be erased. Then eq.(5) is obtained.

$$a_X = a_F + (l_X - l_F)\frac{a_F - a_A}{l_F - l_A} \quad (5)$$

where $l_X - l_F$ is the distance from F to X, $l_F - l_A$ is the distance from A to F. Eq.(5) indicated that the instantaneous acceleration a_X is calculated by Eq.(5) with the measured instantaneous accelerations a_A and a_F.

Fig.7 shows the comparison between the calculated acceleration on midship by Eq.(5) using accelerations measured on the stem and stern and the acceleration measured on the midship position. From the results, it is confirmed that the calculated result is good agreement with the measured results.

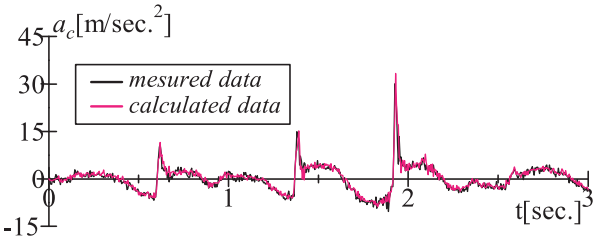

Fig.7 Time histories of measured and calculated results at *s.s.*5.0 in irregular wave. (sea state 4, *Fn*=0.51, Ship A)

3.5 Making irregular waves

Eq.(6) is ISSC spectrum, and Eq.(7) is the relations between significant wave height $H_{1/3}$ [m] and average wave period T_1 [sec].

$$\frac{S(\omega)}{H_{1/3}{}^2 T_1} = \frac{0.11}{2\pi}\left(\frac{\omega T_1}{2\pi}\right)^{-5} \exp\left\{-0.44\left(\frac{\omega T_1}{2\pi}\right)^{-4}\right\} \quad (6)$$

$$T_1 = 3.86\sqrt{H_{1/3}} \quad (7)$$

where ω [rad/sec] is circular frequency of wave, $S(\omega)$ [m^2 sec]is energy density function of wave. To make irregular waves, the spectrum is divided into 100 equally in 0.2~2.5Hz, and a sine wave of each frequency component is superposed. In addition, the phase difference of each frequency component is given as random numbers for each measurement. Table 2 shows the range of wave height for sea state in real scale, and the wave height in this study. The towing speeds in the measurement are 0, 10, 15, 20, 25, 40kts in real scale.

Table 2 Wave conditions of the experiment.

sea state	wave height for seastate [m]	typical wave height for a sea state	average wave period : T_1 [sec.]
3	0.50~1.25	0.70	3.2
		1.00	3.9
4	1.25~2.50	2.00	5.5
5	2.50~4.00	3.00	6.7

4. CHARACTRISTICS OF ACCELERATION

4.1 Effects of Type of Ship

As an estimation method of vertical acceleration on hull, Osumi's chart (Osumi, 1992) and Savitsky's empirical formula (Savitsky et al., 1976) are known. Fig.8 shows the comparisons between the measured results (Ship A) and Osumi's results. The measured results are larger than Osumi's results. It is supposed that Osumis' results does not include the impact acceleration shown in Fig.5, because the object ship is the high speed patrol boat. Fig.9 shows the comparisons between the measured results and Savitsky's results. The measured results are smaller than Savitsky's results. It is supposed that Savitsky's results include large impact acceleration, because the object ships is typical planing hulls which is hard chine straight deep V monohedron without bow flare.

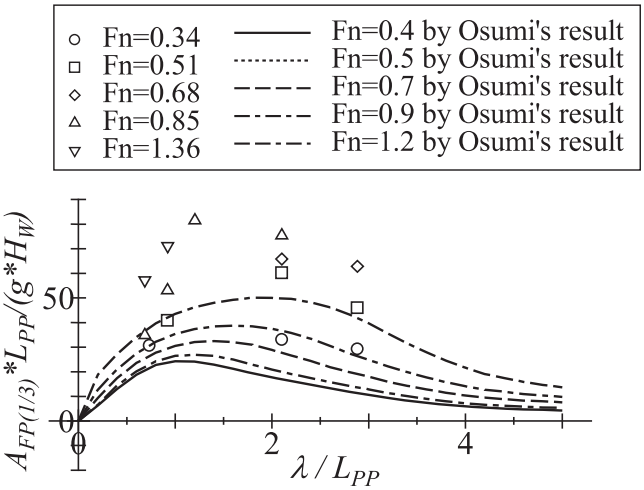

Fig.8 Comparison of non-dimensional significant peak to peak amplitude of acceleration between the measured results and Osumi's results.

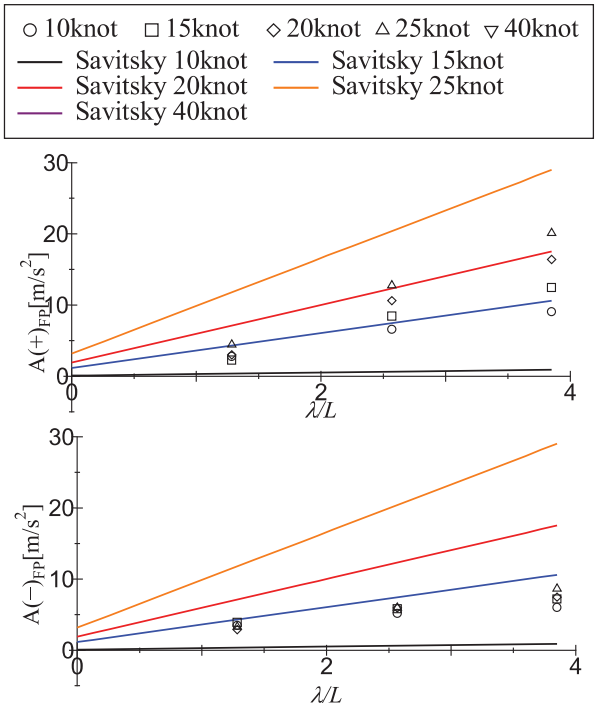

Fig.9 Comparison of average peak value of vertical acceleration between the measured results and Savitsky's results. (upper figure: upward peak value, lower figure: downward peak value)

4.2 Effects of wave length and height

Fig.10 shows non-dimensional average upward or downward peak value of measured vertical acceleration on hull. In the figure, the horizontal axis is the ratio of wavelength to ship length λ/L_{PP}. The wavelength is calculated from $\lambda=g/(2\pi)\times T_1$. Eq.(8) is proposed to fit to the measured results, and the fitted curves are shown the figure.

$$y = B \times x \times e^{-Cx} \qquad (8)$$

To investigate the effect of wave height on the vertical acceleration, the measurement with different wave height, constant forward speed and constant average wave period for Ship A is carried out. Fig.11 shows average upward and downward peak values of vertical acceleration at FP. The horizontal axis is $H_{1/3}/L_{PP}$. From the figure, it is noted that the non-dimension values of upward and downward acceleration are linearly increased with increase of wave height. The same tendency can be seen in the upward acceleration in the regular wave shown in Fig.12 in the condition where the impact acceleration shown in Fig.5 occurs because of increase of wave height or/and forward speed.

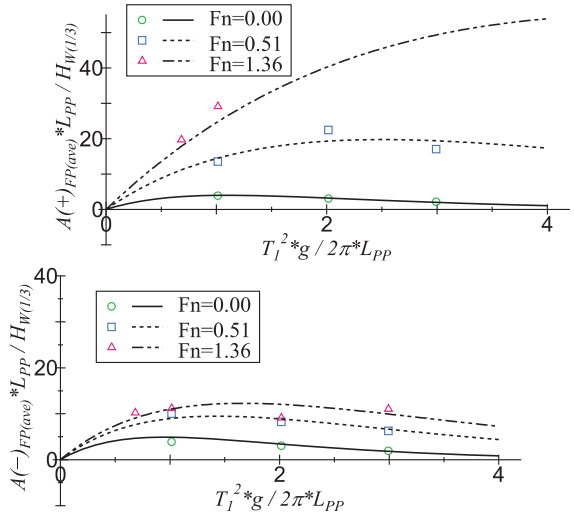

Fig.10 Non-dimensional average peak value of measured vertical acceleration obtained by Eq.(8) for Ship A. (upper figure: upward peak value, lower figure: downward peak value)

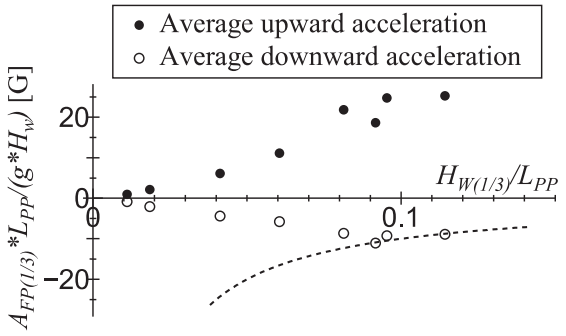

Fig.11 Average upward and downward peak values of vertical acceleration at FP measured for several wave height. (Ship A) In this figure, the black solid line shows the free fall whose acceleration is 1.0 G.

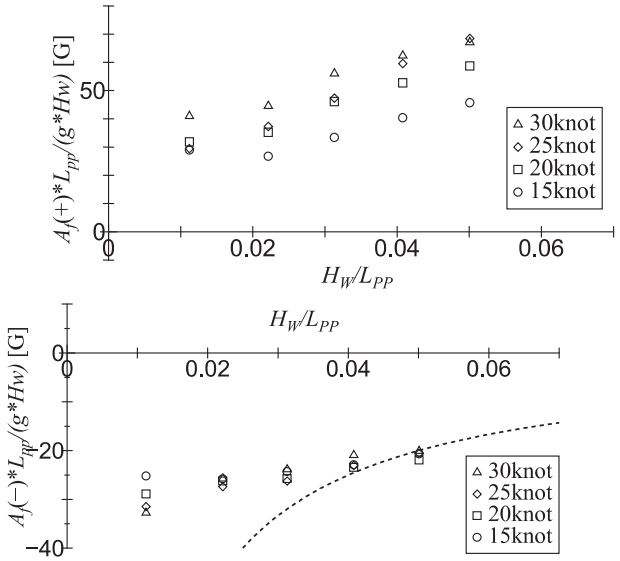

Fig.12 Measured upward and downward peak value of vertical acceleration for wave heights at *s.s.* 10.39 (*Tw*=1.0 sec) (Ship A). (upper figure: upward peak value, lower figure: downward peak value)

4.3 Longitudinal Distribution

Fig.13 shows longitudinal distribution of peak to peak amplitude and peak values of vertical acceleration which is calculated by Eq.(5) with vertical acceleration measured at FP and at *AP*. The horizontal axis is the square station number (AP=0 and FP=10). The vertical acceleration increases with increase of forward speed, and it linearly increase with moving forward of longitudinal position from about *s.s.*=4.0. From the lower figure, it is found that upward peak value is larger than downward peak value, because upward acceleration occurs when bow of ship goes into the water surface. Fig.14 shows the longitudinal position of minimum vertical acceleration. The position is different according to forward speeds or wave periods and moves backward with increase of forward speed or/and wave period.

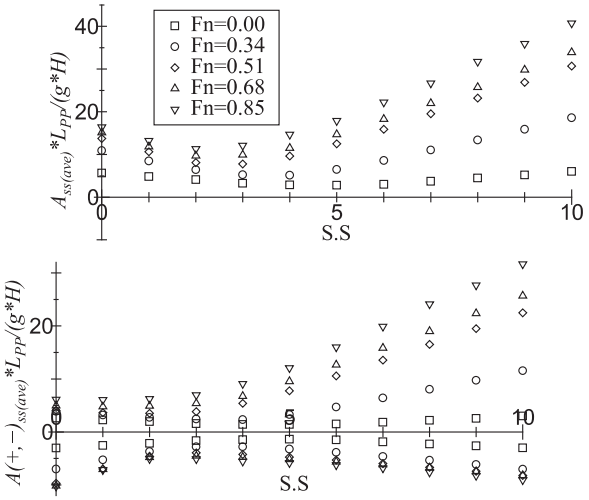

Fig.13 Longitudinal distribution of significant peak to peak value and upward and downward of vertical acceleration on hull. (upper figure: peak to peak value, lower figure, upward and downward of acceleration)

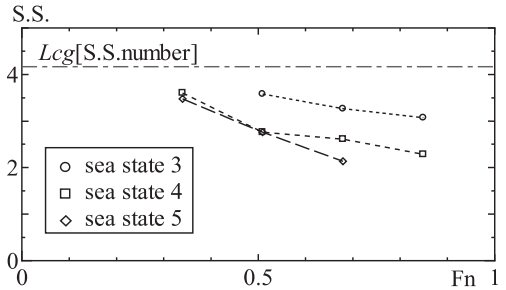

Fig.14 Longitudinal position where amplitude of vertical acceleration is minimum. (Ship A)

Fig.15 shows the non-dimensional value of acceleration shown in Fig.13. Value at arbitrary longitudinal position is divided by the value at FP. To estimate longitudinal

distribution of the acceleration except at Fn=0, Eq.(9), (10) and (11) are proposed as empirical formula.

$$\frac{A_{ss(ave)}}{A_{FP(ave)}} = \begin{cases} \dfrac{s.s.}{10} & (3.0 \le s.s.) \\ \dfrac{(6 - s.s.)}{10} & (s.s. < 3.0) \end{cases} \quad (9)$$

$$\frac{A_{ss}(+)_{(ave)}}{A_{FP}(+)_{(ave)}} = \begin{cases} \dfrac{(3 \times s.s. - 2)}{28} & (3.0 \le s.s.) \\ \dfrac{(10 - s.s.)}{28} & (s.s. < 3.0) \end{cases} \quad (10)$$

$$\frac{A_{ss}(-)_{(ave)}}{A_{FP}(-)_{(ave)}} = \begin{cases} \dfrac{(2 + s.s.)}{12} & (3.0 \le s.s.) \\ \dfrac{(14 - 3 \times s.s.)}{12} & (s.s. < 3.0) \end{cases} \quad (11)$$

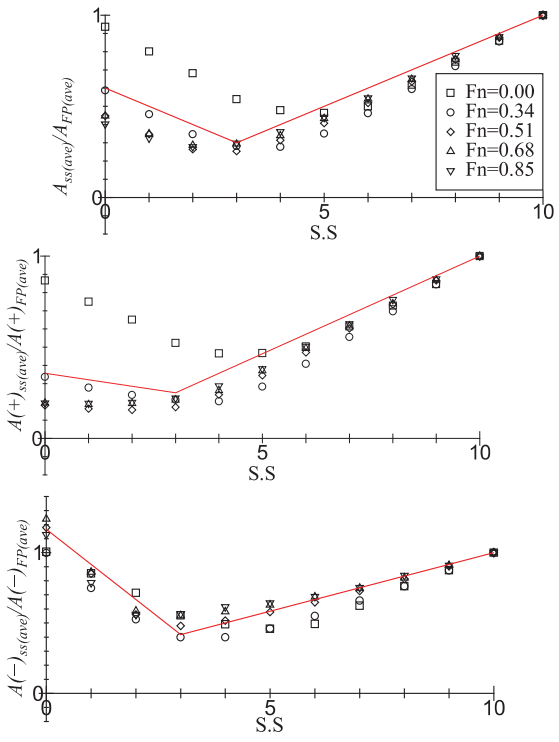

Fig.15 Form of longitudinal distribution of peak to peak value, upward peak value and downward peak value of vertical acceleration on hull in irregular waves. (upper figure: peak to peak value, middle figure: upward peak value, lower figure: downward peak value)

4.4 Effects of Hull Form

Fig.16 shows significant peak to peak value of upward and downward of vertical acceleration on hull with Ship A, B and C. Its horizontal axis is L_{PP}. The extent is different from hull form and vertical acceleration becomes small when deadrise angle becomes large or L_{PP}/B becomes small.

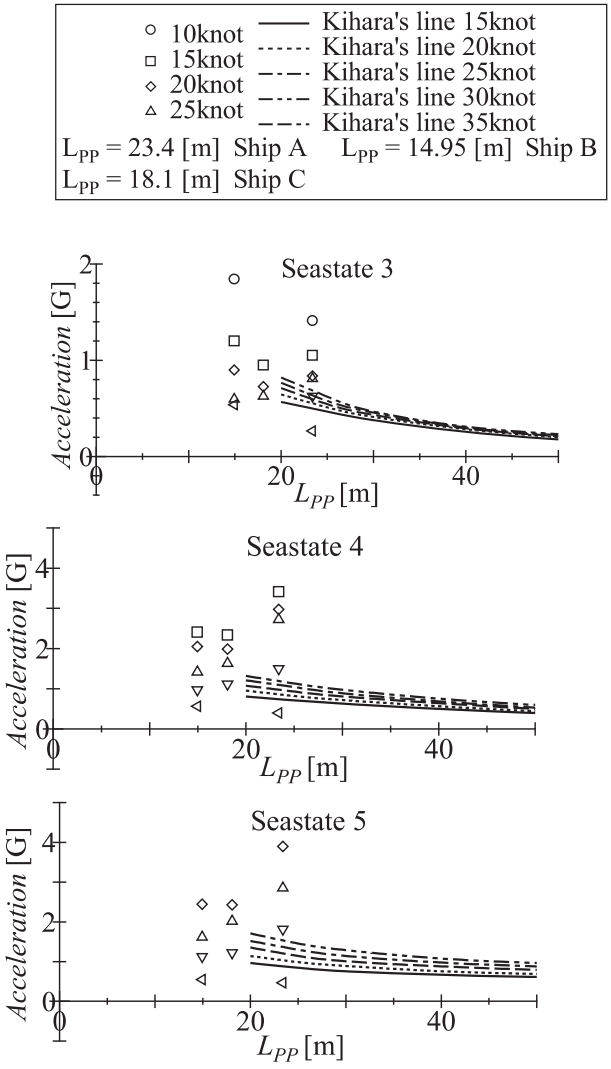

Fig.16 Measured significant amplitude of vertical acceleration on hull at FP vs ship length speed in real scale. (Ship A, B and C) (upper figure: Seastate 3, middle figure: Seastate 4, lower figure: Seastate 5)

4.5 Statistic property

It is well known that the probability density function of amplitudes of acceleration of a displacement type ship in irregular waves can be expressed with Rayleigh distribution of Eq.(12). Rayleigh law describes distribution of the envelope of nomal process. In the case of narrow band spectrum, the envelope can be used as a reasonable approximation of the amplitudes. The maximum likelihood estimate if parameter σ is expressed as Eq.(13).

$$p(x) = \frac{x}{\sigma^2}\exp(-\frac{x^2}{2\sigma^2}) \qquad (12)$$

$$\hat{\sigma} = \sqrt{\frac{1}{2n}\sum_{i=1}^{n} X_i^2} \qquad (13)$$

where X_i is measured datum in time step and n is the number of total datum. The relation among parameter σ, average value, significant value and average 1/10 maximum value of Rayleigh distribution is expressed as Eq.(14).

$$\overline{X} = \sigma\sqrt{\frac{\pi}{2}} = \frac{1}{1.6}X_{1/3} = \frac{1}{2.04}X_{1/10} \qquad (14)$$

Fig.17 shows the comparison of parameter σ, significant value, average 1/10 maximum value obtained from measured results and estimated results by Eq.(14) with the average amplitude of measured data. From upward acceleration in the upper side Fig.17, measured results are larger than estimated results when the average amplitude is larger than 1.0G. On the other hand, downward acceleration in the lower side Fig.17, measured results smaller than estimated results when the average amplitude lager than 0.5G.

Savitsky proposes a probability density function $p(x)$ (Savitsky et al., 1976) as Eq.(15) with exponential distribution.

$$p(X) = \frac{1}{\overline{X}}\exp(-\frac{X}{\overline{X}}) \qquad (15)$$

where $\overline{X}$ is average amplitude of acceleration. The average $1/N$ maximum amplitude of acceleration is proposed as Eq.(16).

$$X_{1/N} = \overline{X}\left(1 + \log_e N\right) \qquad (16)$$

Fig.18 shows comparisons of probability distributions of amplitude of acceleration. The results of Eq.(15) is good agreement with measured results. Fig.19 shows the results of Eq.(16) drowned on the left side Fig.17, and the results is good agreement with the measured results when the average amplitude is larger than 1.0G.

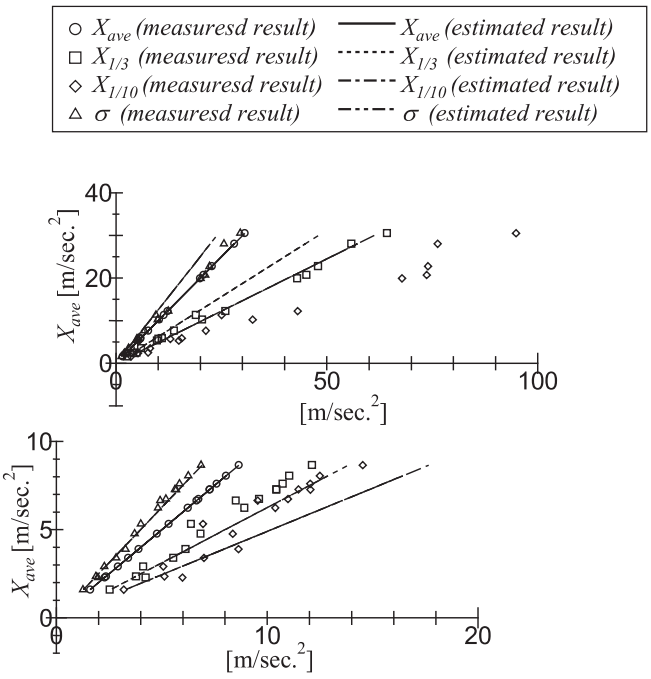

Fig.17 Comparison between measured results and estimated results based on Rayleigh distribution with average value of measured data. (Ship A) (upper figure: upward acceleration, lower figure: downward acceleration)

Fig.20 shows probability distribution of downward peak value of vertical acceleration at FP. The upper figure shows the results when

the average amplitude smaller than 0.5G, and the lower figure shows the results when the average amplitude lager than 0.5G. If average amplitude becomes larger, the mode of amplitude is close to about 1.0G. However when the average is over 0.5G, the mode of amplitude does not becomes much larger than 1.0G and the average amplitude does no becomes larger. Because downward acceleration occurs when ship bow turns rising into falling, bow moves close to free fall when the average is over 0.5G.

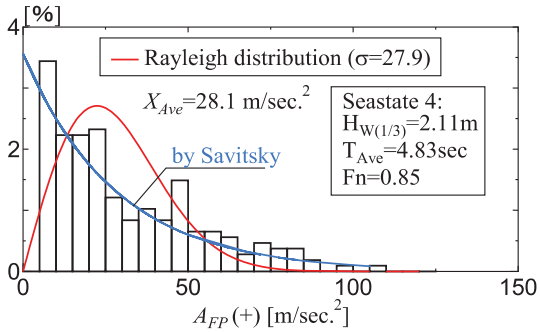

Fig.18 Measured probability distribution of upward peak value of vertical acceleration at FP in irregular wave.

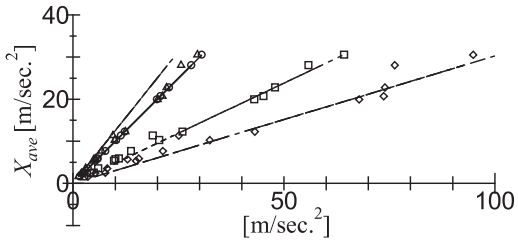

Fig.19 Comparison between measured result and exponential distribution proposed by Savitsky.

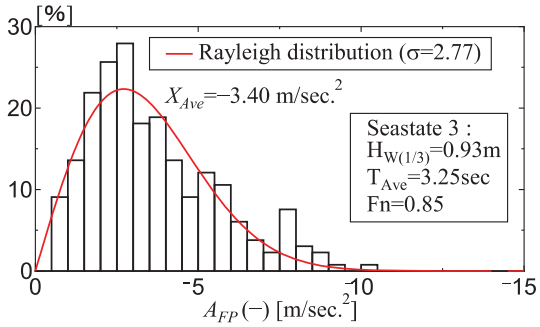

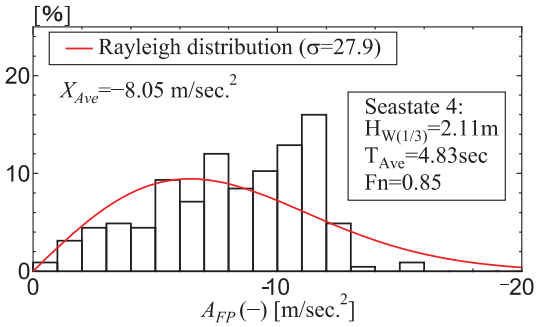

Fig.20 Probability distributions of downward peak value of vertical acceleration at FP in irregular wave. (Ship A)

5. CONCLUSIONS

In this study, the characteristics of vertical acceleration in irregular waves for high speed semi-planing hull is investigated experimentally. The following conclusions are obtained.

1. To measure peak value of impact acceleration accurately, a measurement and analysis procedure is proposed.

2. Based on the measured results, the effects of wave length, wave height and forward speed are indicated and a fitting curve to explain the characteristics of RAO of the acceleration is proposed.

3. Form of longitudinal distribution of the acceleration is discuss, and an empirical equation to express the form expecting at $Fn = 0$ is propose.

4. The vertical acceleration on hull in irregular waves is different with that of

upward and downward acceleration. When impact acceleration doesn't occur, upward acceleration follows Rayleigh distribution and upward acceleration follows that Savitsky's empirical formula. On the other hand, when the average is not over about 0.5G, downward acceleration follows Rayleigh distribution, when over 0.5G, its mode is larger than that of Rayleigh distribution.

Based on the above-mentioned results, the characteristics of the vertical acceleration of a hull can be formulated. It can be possible to estimate vertical on a hull if database of the vertical acceleration for typical hulls are prepared.

6. ACKNOWLEDGEMENT

This work, which was sponsored by JCI (; Japan Craft Inspection Organization), was carried out by Osaka Prefecture University, who is a member of the "Research Committee about the safety of the small high-speed passenger craft of Japan Craft Inspection Organization" which was initiated by JCI.

7. REFERENCES

National Maritime Research Institute, 2007, "Report of research committee of the safety of seat and it equipment for high speed passenger ship".

Osumi, M., 1992, "A design method of a medium-speed boat (continued) (1)", Ship Technology, Vol.45, (in Japanese).

Savitsky, D. and Brown. P. W., 1976, "Procedures for Hydrodynamic Evaluation of Planing Hulls in Smooth and Rough Water", Marine Technology, pp.381-400.

Seakeeping Committee of ITTC, 2011, "Seakeeping Experiments", ITTC Recommended Procedures and Guidelines 7.5-02-07-02.1, p. 6.

Takemoto, H., Naoi, T., Hashizume, Y., Watanabe, I., Nose, Y. and Osumi, M., 1981, "On the Full Scale Measurement of Motions and Impact Loads of a High Speed Patrol Boat in Waves", Transaction of the west-japan society of naval architects, No.61, (in Japanese).